

polymer papers

Rheological and morphological study of the phase inversion in reactive polymer blends

A. Bouilloux and B. Ernst

Elf-Atochem, Cerdato, F-27470 Serquigny, France

and A. Lobbrecht and R. Muller*

Institut Charles Sadron (CRM-EAHP), 4, rue Boussingault, F-67000, France

(Revised 20 November 1996)

The morphology and melt rheological properties were characterized for a polymer blend where the viscosity ratio was changing with time. The reactive phase, an ethylene methyl acrylate (EMA) copolymer containing a diol, was blended in the melt with linear low density polyethylene (LLDPE). Dual continuity was found for the initial morphology of the reactive blends over a broad range of composition in contradiction with the phase inversion rule: $\Phi_A \eta_B = \Phi_B \eta_A$. The influence of blending conditions and annealing on the initial morphology was studied. For a blend where the LLDPE phase is initially dispersed in EMA, the torque and normal force measured in the parallel plate geometry go through a maximum when the morphology becomes co-continuous. © 1997 Elsevier Science Ltd.

(Keywords: polymer blend; morphology; phase inversion)

INTRODUCTION

The wide application of polymer blends has stimulated interest in the prediction of formation of morphologies during mixing of processing in the melt. For two-phase immiscible blends, several parameters are important in determining the final morphology: composition of the blend, shear rate and elongational strain rate during mixing, viscosity and elasticity of both phases, interfacial tension, and time of mixing.

An empirical equation has been proposed to predict the point of dual phase continuity, based only on the blend composition and viscosity ratio^{1,2}:

$$\frac{\Phi_A \eta_B}{\Phi_B \eta_A} = 1 \quad (1)$$

where Φ_A and Φ_B are the volume concentrations of phases A and B, and η_A and η_B their viscosities. If the ratio in equation (1) is lower than 1, phase A should form the dispersed phase in a continuous matrix of B, whereas B should be dispersed in A for values higher than 1. According to the above condition, the component with the higher viscosity can be dispersed in the lower viscosity component, even if it is present at a higher volume fraction in the blend. For non-Newtonian liquids, it has been suggested³ that the viscosities should be taken at the shear rate of the flow. If the viscosity ratio is shear rate dependent and the shear rates are non-uniform in the mixing device, determination of the viscosity ratio in equation (1) may appear somewhat arbitrary. Though it does not take into account important effects like non-uniformity of shear rates in mixing devices, interfacial effects or melt elasticity,

equation (1) was found satisfactory to describe phase inversion for various systems³⁻⁵ where the components have approximately the same viscosity, whereas significant deviations were found for viscosity ratios diverging from unity⁶.

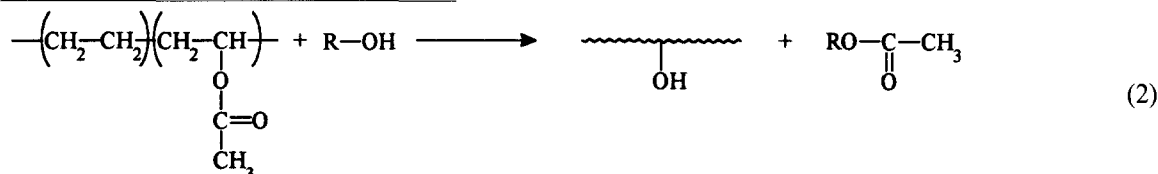
Usually, the morphology of immiscible polymer blends is characterized by scanning electron microscopy (SEM). If the morphology is not uniform on a scale larger than that of the micrographs, the results may be non-representative of the bulk material. Indirect techniques, like solubility⁷ or permeability⁸ measurements, can complement the information provided by SEM, especially for complex co-continuous morphologies. To follow the rheological properties of the blend can be an alternative way to characterize morphological changes. This method has been mainly used during the synthesis of high-impact polystyrene, where the viscosity of the (polymerizing) styrene phase increases with time. A discontinuity of the viscosity *versus* time curve could be observed⁹⁻¹¹, which was found to correspond to phase inversion.

It was the purpose of the present study to correlate the evolution of morphology and rheological properties for a polymer blend in the melt for which the viscosity ratio is changing with time. Starting with a dispersion of the more viscous component, we will let the viscosity of the initially less viscous matrix continuously increase with time, while the blend is submitted to a controlled shear flow. This will require the choice of an appropriate reactive system. According to equation (1), dual phase continuity and phase inversion should occur for a given value of the viscosity ratio. Our aim is then to correlate the measured rheological properties to the morphological changes, which will be followed by quenching the system at different values of the viscosity ratio.

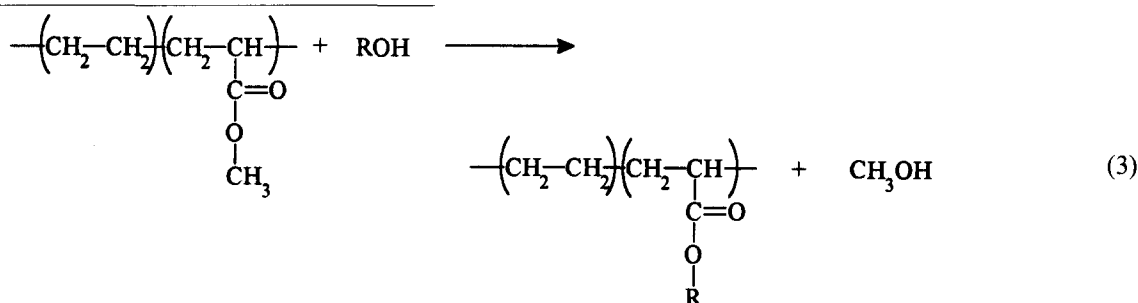
* To whom correspondence should be addressed

EXPERIMENTAL TECHNIQUES AND SAMPLES

The experiment we intend to realize involved several steps for the blend preparation: the reactive phase should be prepared first; in a second step, this phase should be blended with the second, non-reactive phase. During these first two steps, the viscosity of the reactive phase should remain constant. It is only during the last step,



where the blend is submitted to the controlled flow in the rheometer, that the viscosity of the reactive phase should increase with time. Before detailing the materials which



have been chosen, we briefly describe the devices used for the sample preparation and rheological tests.

Experimental devices

The reactive phase and the blends were prepared by melt-blending in a Brabender mixing chamber (Haake Buchler System 90) using the roller blade attachment for viscous materials. About 50 g of material can be prepared in this chamber, and the torque can be measured throughout the test.

The rheological properties of the phases were characterized by dynamic mechanical measurement using a Rheometrics Mechanical Spectrometer RMS 605, in parallel plate geometry. The specimen dimensions were usually 2 mm in thickness and 50 mm in diameter.

The rheological and morphological changes induced by the evolution of viscosity of the reactive phase were studied during flow at constant shear rate, using the same geometry (parallel plates). Therefore, the shear rate is not uniform as in cone-and-plate geometry, but depends linearly on the radius (the values of shear rate which will be given below are those taken at the outer radius). We nevertheless chose the parallel plate geometry, since it allows one to minimize phase deformation before the measurement. On the other hand, at a typical shear rate of 1 s^{-1} in the cone-and-plate geometry, the normal force values exceeded the measuring range of the transducer, and secondary flows were observed.

Reactive phase

A crosslinking reaction, which leads in the first stage to an increase in the average molecular weight of the polymer chains, was used. However, the extent of the reaction had to be kept below the gel point, where the material becomes a viscoelastic solid. Beyond the gel

point, if the crosslinked phase is the dispersed one, no more morphological changes will be induced by the flow. On the other hand, if gelation occurs for the continuous phase, the blend can no longer experience a steady shear flow.

The transesterification, reaction (2), between an ethylene vinyl acetate (EVA) copolymer and a mono-alcohol has been described in the literature¹²:

If an ethylene methyl acrylate (EMA) copolymer is used instead of EVA, the transesterification reaction leads to grafting of the alcohol group on to the main chain according to:

By using a diol, this reaction leads to crosslinking.

The following reactive system has been chosen: the polymer is an EMA random copolymer supplied by Elf-Atochem under the commercial name Lotryl 28MA07. The total weight average molecular weight M_w of this polymer is $100\,000 \text{ g mol}^{-1}$ and the molar content of acrylate groups is 11.3% (28% in weight). The melting temperature was found to be around 65°C . The transesterification reaction involves a low molecular weight diol (1,4-butanediol) and dibutyltin dilaurate (DBTDL) as a catalyst¹².

The reactive phase was prepared by introducing the diol and the catalyst into the molten EMA in the Brabender mixer. The main parameters controlling the

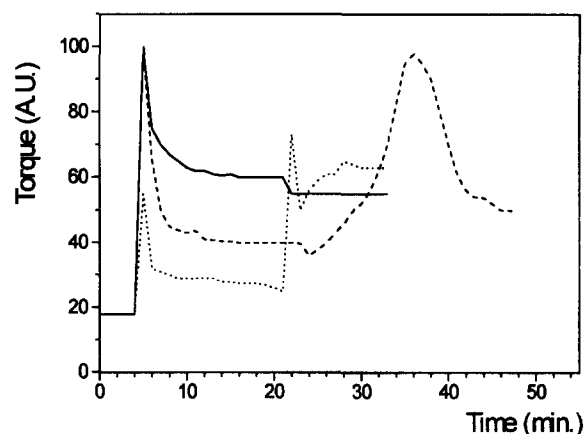


Figure 1 Torque (arbitrary units) as a function of time in the Brabender mixing chamber for the reactive EMA phase ratio with $[\text{alcohol}]/[\text{acrylate}] = 1/5$ at different temperatures: solid line, 80°C ; dashed line, 150°C ; dotted line, 230°C

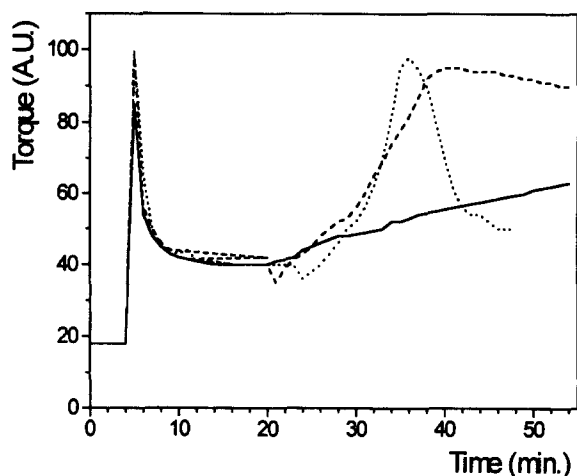


Figure 2 Torque (arbitrary units) as a function of time in the Brabender mixing chamber at $T = 150^{\circ}\text{C}$ for the reactive EMA phase at different values of the ratio [alcohol]/[acrylate]: solid line, 1/20; dashed line, 1/10; dotted line, 1/5

kinetics of the transesterification reaction are the temperature, the concentration of catalyst and the molar ratio [alcohol]/[acrylate] of alcohol over acrylate groups. The molar ratio of DBTDL over acrylate groups has been fixed to 1/100 and three different values of the ratio [alcohol]/[acrylate] were tested: 1/5, 1/10 and 1/20. The quantities of added reagents were then of the order of 1 g, which allowed us to adjust the concentrations of diol and catalyst with sufficient precision.

Due to the low melting temperature of the EMA copolymer, the mixing temperature could be lowered to about 80°C , where the kinetics of the reaction is negligible during the usual mixing times. This is confirmed in *Figure 1*, where the torque measured on the Brabender has been plotted as a function of time for three temperatures and the highest concentration of diol. At 80°C , the torque remained constant after the initial decrease due to the melting of EMA. At higher temperatures, the torque and viscosity increased with time due to the crosslinking reaction. If the gel point is exceeded, a maximum in the torque was observed, due to powdering of the crosslinked material in the mixing chamber.

Throughout the present study, the reactive EMA phase was obtained by melt-blending the reagents at 80°C and 50 rev min^{-1} during 10 min in the Brabender mixing chamber. The material was then compression moulded in the form of 2 mm thick plates, from which either samples for the rheological tests, or pellets for further blending with the non-reactive phase, were obtained. The torque measurements of *Figure 1* have been confirmed by dynamic mechanical data obtained at 140°C on reactive EMA prepared as described above. The G' and G'' versus frequency curves were found to be identical to those obtained on the same material prepared without catalyst, thus confirming that the reaction did not take place in the mixing chamber.

Non-reactive phase

The second, non-reactive phase had to satisfy several conditions: it should be immiscible with EMA copolymer, and its melting or glass transition temperature should be low enough so that the blending with the reactive phase can be performed without crosslinking. On the other hand, the viscosity of this phase should be

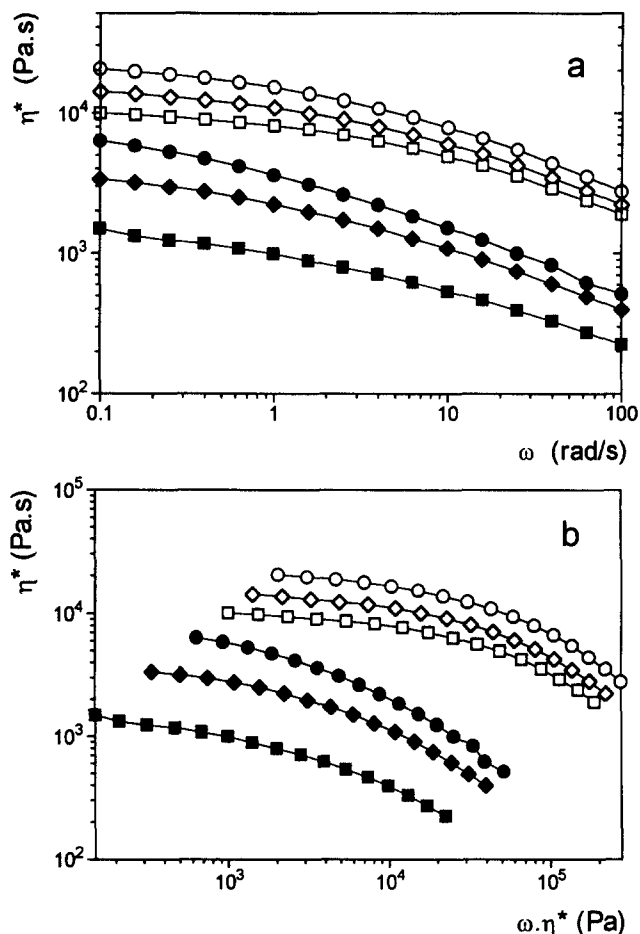


Figure 3 Dynamic viscosity η^* versus (a) frequency ω and (b) the product $\eta^* \times \omega$ for PE (open symbols) and reactive EMA (solid symbols) at different temperatures: 160°C (●, ○); 180°C (◆, ◇); 200°C (■, □)

higher than the initial viscosity of the EMA phase, so that EMA forms the continuous phase in the initial blend morphology. Finally, the existence of selective solvents would facilitate the morphological analysis.

Linear low density polyethylene (LLDPE) proved to be an adequate choice with respect to the above conditions. First, it was found to be immiscible with EMA for the concentration of acrylate groups of Lotryl 28MA07. On the other hand, due to the low melting temperature of LLDPE, the preparation of the blends can be realized at a moderate temperature, for instance in the range $140\text{--}150^{\circ}\text{C}$. It has to be pointed out that the same type of experiments could also be carried out by using polypropylene with a low melting temperature ($T_m = 130\text{--}135^{\circ}\text{C}$) as the non-reactive phase. *Figure 2* shows the time dependence of the torque in the Brabender mixer for the reactive EMA phase, at 150°C and for three concentrations 1,4-butanediol. It is found that for the lowest concentration of diol, the crosslinking reaction of EMA is slow enough to allow mixing during about 15 min without significant increase of viscosity.

Due to the wide range of commercially available resins, the condition on the initial viscosity ratio between both phases could be easily satisfied: we chose a LLDPE from Dow Chemical (Dowlex NG5055E with a density of 0.923 and MFI of 0.7), which will be later referred to as PE. *Figure 3* shows the dynamic viscosity of this polymer as a function of frequency (*Figure 3a*) and as a function of the product of frequency times the dynamic

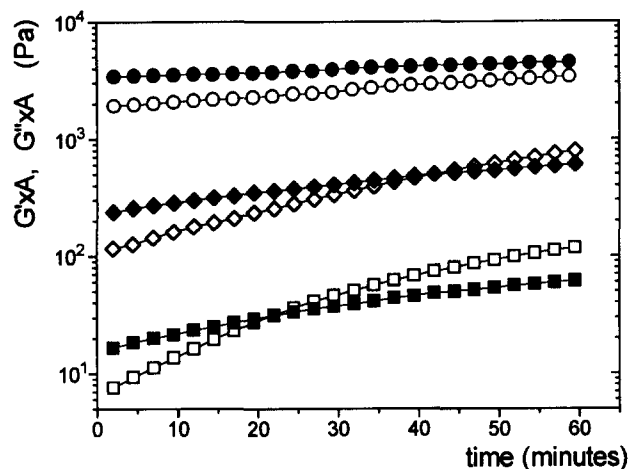


Figure 4 Dynamic moduli G' (\circ , \diamond , \square) and G'' (\bullet , \blacklozenge , \blacksquare) of EMA as a function of reaction time at different temperatures: 160°C (\bullet , \circ , $A = 0.1$); 180°C (\blacklozenge , \diamond , $A = 0.1$); 200°C (\blacksquare , \square , $A = 0.01$)

viscosity (Figure 3b) at three temperatures, compared to that of EMA before the transesterification reaction. According to the Cox–Merz rule, these plots are equivalent to shear viscosity *versus* shear rate (Figure 3a) and shear viscosity *versus* shear stress (Figure 3b) curves.

Finally, EMA can be dissolved in chloroform at 50°C, whereas LLDPE is insoluble under these conditions. This means that, for the morphological analyses, it was possible to dissolve the EMA phase selectively and to identify unambiguously both phases, for all blends where PE forms the continuous phase, or for co-continuous morphologies. At the same time, the dissolution test showed whether or not the EMA phase remained soluble and, therefore, allowed us to confirm if the crosslinking reaction was indeed kept below the gel point. Since no selective solvent could be found for PE at temperatures lower than the melting temperature of EMA, morphologies of blends where PE was dispersed in an EMA matrix were observed without solvent treatment. However, the solvent treatment helped to confirm these morphologies since the corresponding blends completely dissolved in chloroform. It has been suggested in the literature^{6,13} to define a degree of co-continuity from extraction data for each component with a selective solvent as a function of blend composition, the maximum degree of co-continuity (equal to 1) being obtained when each component is entirely soluble in its selective solvent. In our case, extraction data are only available for the EMA phase. The weight fraction of EMA present in the blend that was actually extracted by the solvent treatment was usually lower than 1 and increased with EMA content, in agreement with previous data from the literature¹³. The fact that all EMA was not extracted does not seem to be due to crosslinking, since blends containing more than 70% EMA, and prepared under the same mixing conditions, remained entirely soluble in chloroform.

RHEOLOGICAL CHARACTERIZATION OF THE TRANSESTERIFICATION REACTION

The choice of the experimental parameters of the phase inversion experiment, based on equation (1), required a precise knowledge of the viscosity of the reactive EMA

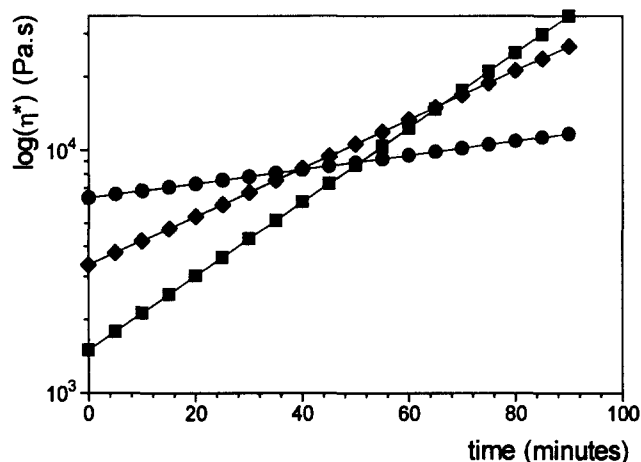


Figure 5 Dynamic viscosity of EMA as a function of reaction time at $\omega = 1 \text{ rad s}^{-1}$ and different temperatures: 160°C (\bullet); 180°C (\blacklozenge); 200°C (\blacksquare)

phase as a function of temperature, shear rate and time. A further condition came from the requirement that the gel point should not be exceeded during the blend preparation and the phase inversion experiment.

Estimation of gelation time

The dynamic moduli and viscosities of EMA were measured as a function of reaction time at various temperatures and frequencies. The dynamic moduli as a function of reaction time for the lowest diol concentration ([alcohol]/[acrylate] = 1/20) are shown in Figure 4 at three temperatures (160, 180 and 200°C). Both G' and G'' increased with reaction time. At 200 and 180°C, a crossover between the two moduli was observed after 22 and 40 min, respectively. At 160°C, the moduli only slightly increased during the time of measurement (60 min) and no crossover was observed. At 140°C, the moduli remained constant within experimental error up to a 60 min reaction time.

It has been shown¹⁴ that the gel point can be identified in a crosslinking process from dynamic mechanical measurements on the reaction medium. For stoichiometric reaction media, the crossover between G' and G'' has been found to correspond precisely to the gel point, whereas for unbalanced conditions^{15,16}, G' and G'' are in a ratio usually between 0.6 and 1. At the gel point, both G' and G'' follow a power law with the same exponent, so that their ratio is independent of frequency. As a first approximation, we used the crossover point between the dynamic moduli at $\omega = 1 \text{ rad s}^{-1}$ to estimate the reaction time at the gel point as a function of temperature. This was also the maximum time for the phase inversion experiments keeping the reactive phase in the liquid state, which was confirmed by etching in chloroform.

Viscosity of EMA as a function of reaction time

We assume throughout this study that the Cox–Merz rule is verified for both phases, which means that we may use equally well the shear viscosity η at a given shear rate $\dot{\gamma}$ appearing in equation (1), or the dynamic viscosity $\eta^* = \sqrt{G'^2 + G''^2}/\omega$ at a frequency $\omega = \dot{\gamma}$ measured by dynamic mechanical analysis.

Since the viscosity was a function of both frequency and reaction time, the viscosity as a function of time at a given frequency and temperature was obtained in the

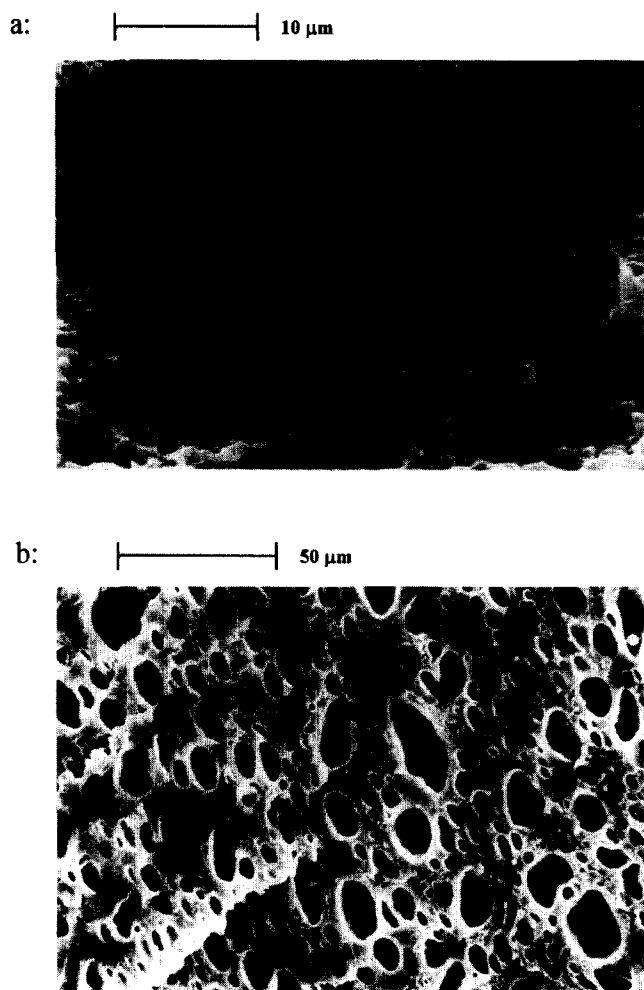


Figure 6 SEM micrograph of blend PE/EMA 7/3 mixed during 6 min at 50 rev min^{-1} (a) without and (b) after etching in chloroform at 50°C

following way: several consecutive frequency sweeps were carried out at a fixed temperature. Selecting a given frequency, the data (one value per frequency sweep) were then plotted as a function of reaction time. By repeating the procedure for all frequencies and various temperatures, curves like those given in *Figure 5* were obtained in the range $0.1 < \omega < 100 \text{ rad s}^{-1}$ for $T = 140, 160, 180$ and 200°C . At 140°C , no viscosity change could be observed up to 60 min reaction time.

PREPARATION AND CHARACTERIZATION OF REACTIVE BLENDS

Preparation of reactive blends

As indicated above, the reactive EMA phase was prepared first by melt blending the diol and the catalyst with the copolymer at 80°C during 10 min, and pressing the obtained material into 2 mm thick plates at the same temperature. These plates were then pelletized and blended with PE in different concentrations in the Brabender mixer during 6 min $T = 140^\circ\text{C}$ and 50 rev min^{-1} . The molten blend was then immediately pressed in the form of 2 mm thick plates at 140°C during 5 min. From these plates, specimens for morphological analyses and for the phase inversion experiments in the parallel plate rheometer were obtained. Densities in the melt of both phases are very close, so that we can identify volume with weight concentrations. No viscosity change

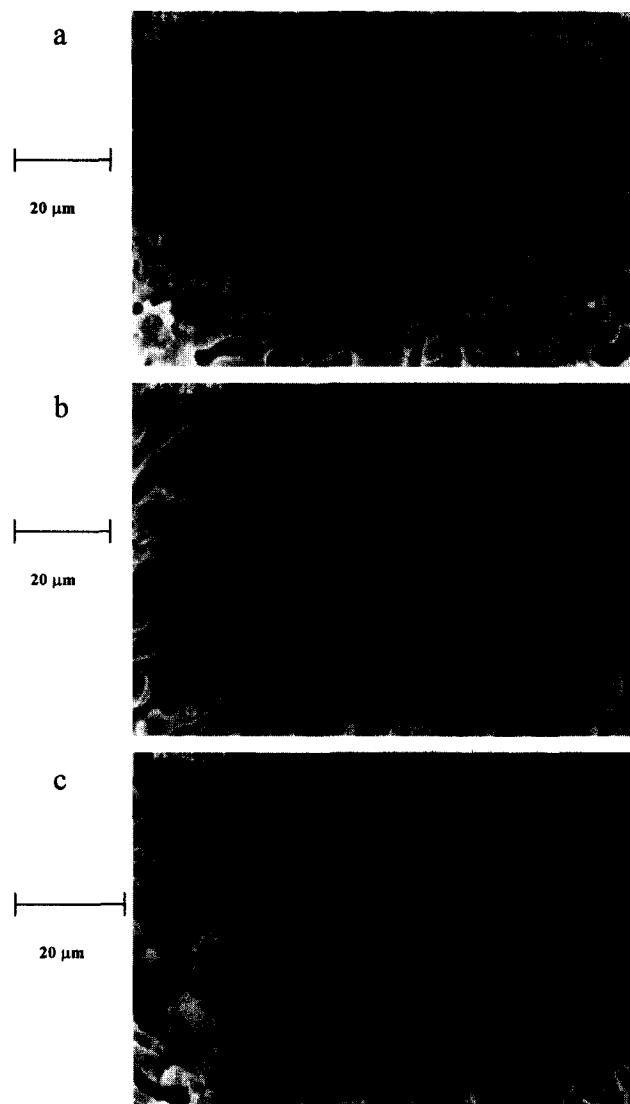


Figure 7 SEM micrographs of blends PE/EMA: (a) 3/2; (b) 1/1 and (c) 2/3 mixed during 6 min at 50 rev min^{-1} after etching

of the reactive EMA phase should occur under these processing conditions, since viscous heating as measured by taking directly the temperature of the melt after blending is found to be negligible.

For the morphological analyses, we used a scanning electron microscope (Cambridge Stereoscan 120) with about 20 kV acceleration voltage. Morphologies were observed on a fracture surface after cooling the sample in liquid nitrogen. For each observation, two specimens were prepared: one was observed directly after cryofracture, the other was further placed for 1 h in chloroform at 50°C , under agitation, to dissolve the EMA phase, and dried *in vacuo* during 12 h to remove the residual solvent. On the other hand, for each blend, several specimens were taken at different places of the compression moulded plate. The morphology of these specimens was always found to be almost identical, thus confirming the homogeneity of morphology for our mixing conditions.

Initial morphology of reactive blends

The shear rates or shear stresses in the mixing chamber are not uniform and difficult to estimate. However, *Figure 3* shows that the viscosity ratio between PE and

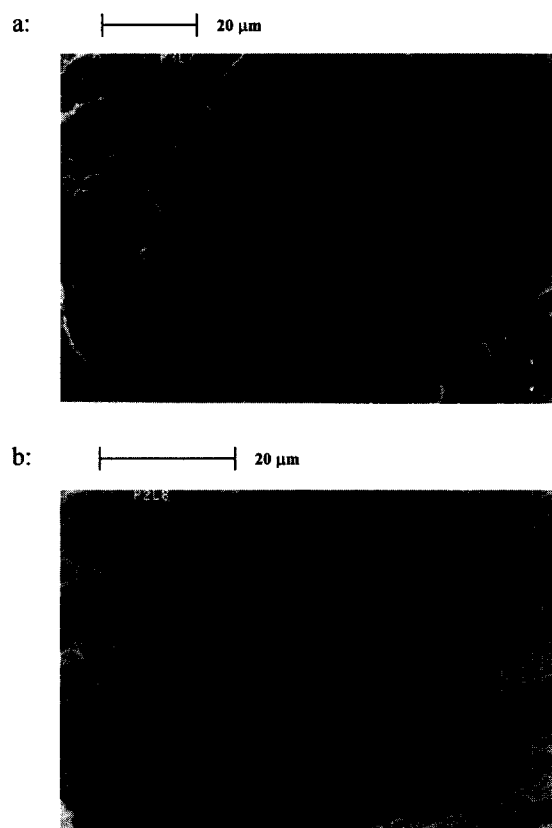


Figure 8 SEM micrographs of blends PE/EMA: (a) 3/7 and (b) 1/4 mixed during 6 min at 50 rev min^{-1} without etching

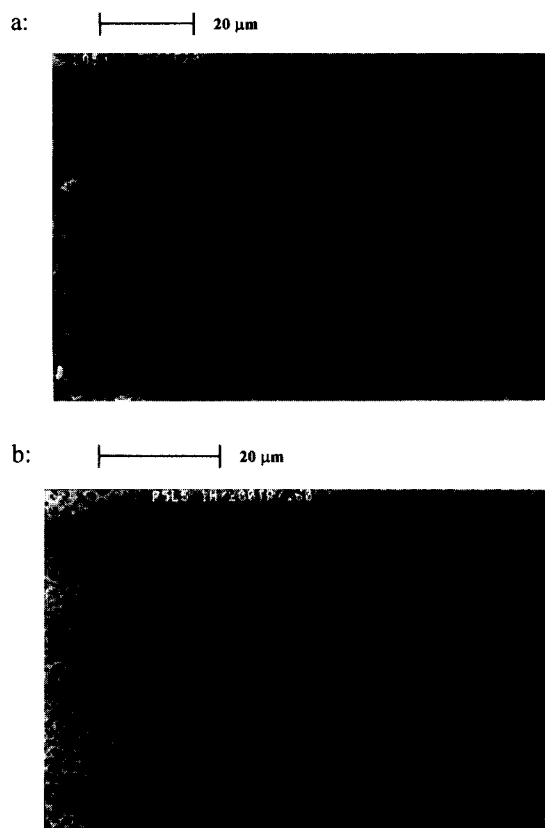


Figure 9 SEM micrographs of blend PE/EMA 1/1 mixed during (a) 6 min at 200 rev min^{-1} and (b) 1 h at 200 rev min^{-1} after etching

EMA (before crosslinking) taken at constant shear rate is almost independent of shear rate in the range corresponding to the (roughly estimated) shear rates in Brabender ($10\text{--}100 \text{ s}^{-1}$). For temperatures lower than 180°C , this ratio is close to 5. If the viscosity ratio is taken at constant shear stress, its value is no longer constant, but increases with shear stress from around 5 to about 15 at shear stresses of about 10^5 Pa . Despite the strong dependence of viscosity ratio on shear stress, which could induce a wide range of morphologies, these were found to be very uniform in the whole samples taken out of the mixing chamber. According to the phase inversion rule, equation (1), and for viscosity ratios higher than 5, EMA should form the continuous phase if it is present in a concentration higher than about 17%. To verify if we obtain the expected morphology, a first blend containing 30% EMA (referred to as PE/EMA 7/3) was prepared. The micrographs taken with and without solvent extraction are shown in *Figure 6*. Whereas the image obtained without extraction (*Figure 6a*) is difficult to interpret in terms of morphology, *Figure 6b* clearly shows the holes corresponding to the dissolved EMA phase, which forms a dispersion in the continuous PE matrix. That the PE phase is continuous is confirmed by the fact that the specimens keep their shape and are not entirely dissolved during etching with chloroform.

This result is in contradiction with equation (1), but the same type of discrepancy has already been observed for polypropylene/polycarbonate blends by Favis and Chalifoux¹⁷. For their systems also, the less viscous phase was still dispersed at concentrations much higher than predicted by equation (1). To be able to induce phase inversion by increasing the viscosity of EMA, we needed an initial morphology where PE was dispersed in

a continuous EMA phase. Therefore, we prepared blends with increasing concentrations of EMA (40, 50, 60, 70 and 80%). Up to 60% EMA content, the specimens did not entirely dissolve in chloroform, thus indicating that the PE phase remained continuous. The corresponding morphologies shown in *Figure 7* confirm a co-continuous structure for these blends (PE/EMA 3/2, 1/1 and 2/3). For concentrations of EMA higher than 70%, the whole specimens dissolve in chloroform, indicating that PE is now dispersed in EMA. This is confirmed by the micrographs in *Figure 8*, obtained without etching and showing (PE) domains dispersed in a continuous (EMA) matrix.

The main result of this morphological analysis is the large concentration range where the phases are co-continuous and the very low concentration of the high viscosity phase at which it is finally dispersed in the low viscosity matrix. Though similar results are observed in the literature, this is in strong contradiction with the empirical phase inversion rule and existing theories¹⁸.

The question therefore arises as to what extent the observed morphologies depend on the mixing history (shear rate and mixing time). For one particular concentration (PE/EMA 1/1) we increased the shear rate in the mixing chamber up to 200 rev min^{-1} , keeping the mixing time constant at 6 min. The morphology obtained after solvent extraction, shown in *Figure 9a*, is still co-continuous, but with a smaller characteristic size than the one obtained at smaller shear rates (50 rev min^{-1} , *Figure 7b*). We then increased the mixing time from 6 min to 1 h at 200 rev min^{-1} . The resulting morphology shown in *Figure 9b* is again co-continuous, but with a still smaller characteristic size. The specimens corresponding to the micrographs in *Figure 9* were not

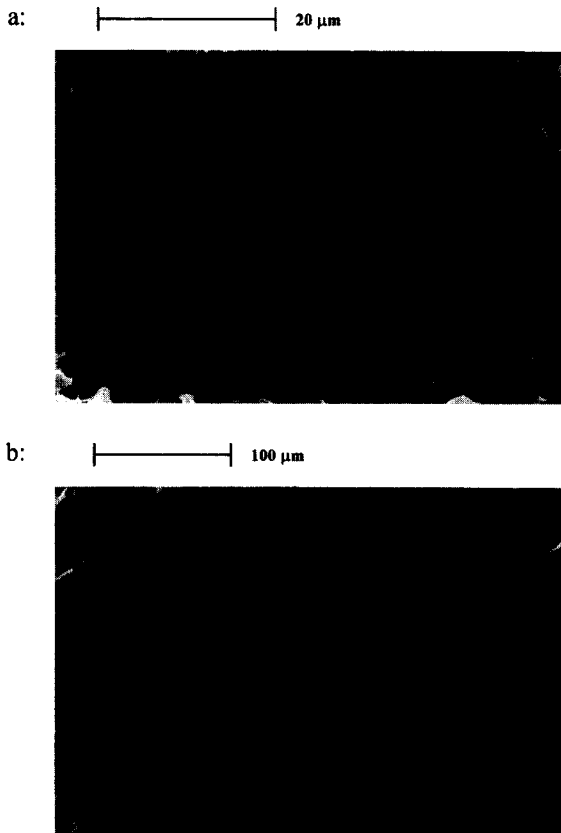


Figure 10 SEM micrographs of blend PE/EMA 1/1 mixed during 6 min at 50 rev min⁻¹ after annealing at 160°C during (a) 3 h without etching and (b) 47 h after etching

entirely soluble in chloroform, this confirming that the PE phase remains continuous in the blends.

It appears that the dual phase continuity obtained for our blends over a wide range of composition does not depend on the mixing history. Increasing the shear rate and mixing time does not lead to a dispersion of the higher viscosity component, but only affects the characteristic dimension of the co-continuous structure, a finer structure being obtained at higher shear rates and longer mixing times.

Influence of annealing

Finally, one may ask whether the morphologies obtained after mixing are stable or not during a subsequent annealing of the blend (kept at rest in the molten state). If the co-continuous morphologies (e.g. *Figure 7b*) are considered to a first approximation as a set of fibres of radius R , these may break into small droplets due to growing disturbances driven by interfacial tension¹⁹ which would eventually lead to a dispersion type morphology¹⁸. The time required for break up of a long fibre of initial radius R_0 embedded in a matrix of viscosity η_m can be estimated by assuming that the initial amplitude of disturbances is due to thermal fluctuations²⁰. The expression of the breaking time is then²¹

$$t_b = \frac{\eta_m R_0}{\sigma \Omega_m} \ln \left(10^{23} \frac{\sigma R_0^2}{T} \right) \quad (4)$$

where σ is the interfacial tension, T is the temperature, and Ω_m is a dimensionless growth rate depending on the viscosity ratio p between fibre and matrix. Both σ and Ω_m

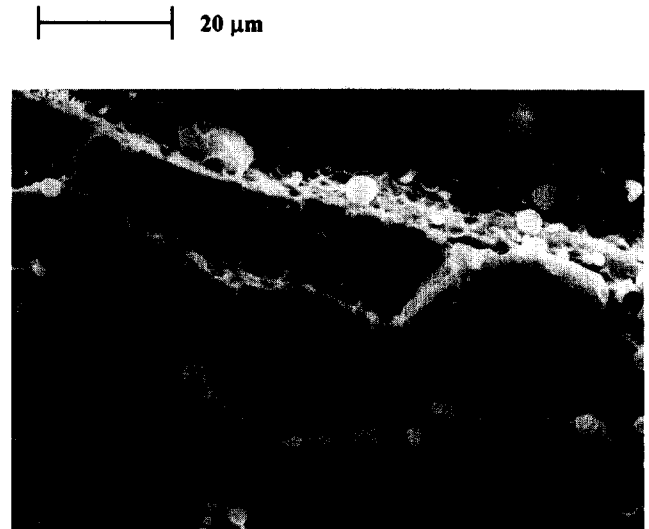


Figure 11 SEM micrograph of blend PE/EMA 3/7 mixed during 6 min at 50 rev min⁻¹ after annealing at 160°C during 2 h without etching

are unknown, but since we were interested here in the order of magnitude of the annealing time we should take to observe possible morphological changes, we took $\sigma \cong 10^{-3} \text{ N m}^{-1}$ and $\Omega_m \cong 0.1$, which is the value for $p = 1$ (in our system the phases have of course different viscosities, but for co-continuous structures it is difficult to determine what phase should be taken for the fibre). The break up time estimated in this way is of the order of 50 min.

The morphology of the blend PE/EMA 1/1 was characterized as a function of annealing time at a temperature close to 150°C. For short annealing times (around 10 min) the initial morphology (*Figure 7b*) remained unaffected, in agreement with the above estimation of the break up time. The morphologies obtained for longer annealing times (3 and 47 h) are shown in *Figure 10*. It should be noticed here that to prevent any viscosity changes in the EMA phase for these annealing tests, blends with non-reactive EMA (without diol and catalyst) were specially prepared. It has also been verified for blends of various compositions prepared in standard conditions (without annealing) that removing the diol and the catalyst has no influence on the obtained morphology.

Figure 10 shows that, after annealing, the structure remains co-continuous with a characteristic dimension (e.g. the average fibre diameter) increasing with annealing time: initially of the order of 5 μm , it increases up to about 30 μm after 3 h and 100 μm after 47 h. On the other hand, a secondary structure remains present in each phase of the growing co-continuous morphology: *Figure 10a* obtained without solvent treatment shows small PE inclusions in the EMA phase, whereas *Figure 10b* after extraction of EMA shows small holes corresponding to dispersed EMA particles in the remaining PE phase. The sizes of these secondary particles are of the same order in both phases, and seem to be independent of annealing time and close to the initial fibre diameter. Similar morphologies were reported by Favis and Chalifoux¹⁷, apparently without annealing.

The phase inversion theory of Metelkin and Blekht¹⁸, which predicts a phase inversion criterion close to equation (1)²², is actually based on the assumption of fibres generated by the flow, fibres of polymer A in a

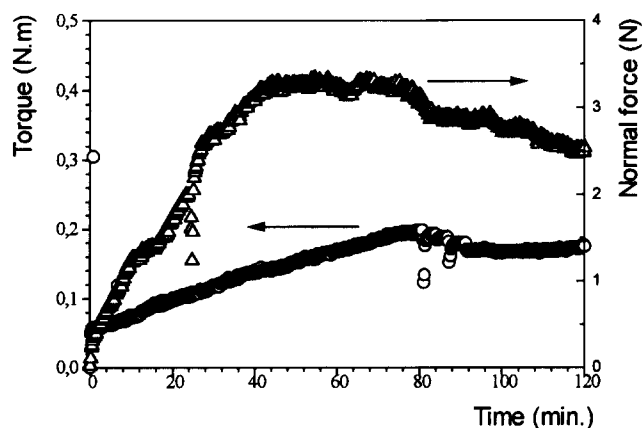


Figure 12 Torque (○) and normal force (△) in the parallel plate rheometer as a function of time for blend PE/EMA 3/7 at $T = 180^{\circ}\text{C}$ and $\dot{\gamma} = 0.4\text{ s}^{-1}$

matrix of polymer B and fibres of polymer B in a matrix of polymer A being both present. Depending on the viscosity ratio of the phases, one type of fibre will break first and the corresponding fibre material will form the dispersed phase. Of course, the assumption of long fibres (periodic instabilities only grow on cylinders with aspect ratio higher than 15²³) of one or the other type is only a crude approximation for the type of co-continuous structures we actually obtained (Figure 7). Our results seem to indicate that these co-continuous morphologies are quite stable and do not break up during flow, and also during annealing at rest. After very long annealing times, these morphologies grow in size, but remain co-continuous in their structure. However, some break up of the initial fibres nevertheless occurs, ending up in a composite fine structure (each phase containing small dispersed inclusions of the other phase).

We also annealed blends where the initial morphology was of the dispersed type. The micrograph in Figure 11 for PE/EMA 3/7 shows only minor changes of the morphology upon annealing. The structure remains of the dispersed type with a slight increase in the dimensions of dispersed droplets, which may be due to coalescence of some particles initially close to each other.

RHEOLOGICAL AND MORPHOLOGICAL STUDY OF THE PHASE INVERSION

Since neither annealing nor increasing the shear rate and mixing time was able to produce a dispersion of PE in EMA for PE concentrations higher than 30%, we focused on the blend PE/EMA 3/7 for the experiment in which phase inversion is induced by increasing the viscosity of EMA. Samples were sheared in the parallel plate geometry at different shear rates and temperatures. After a certain time of shearing, the specimens were rapidly cooled down to room temperature. Specimens for the morphological analysis were taken close to the outer radius of the sample and prepared as described above, with the fracture surface either perpendicular to the radial or to the tangential direction, the shearing direction being respectively normal to and in the plane of observation. Shear rates were limited to values below 1 s^{-1} , where flow perturbations due to melt elasticity became too important. The torque and normal force were measured throughout the experiment.

As expected, the torque and even more the normal

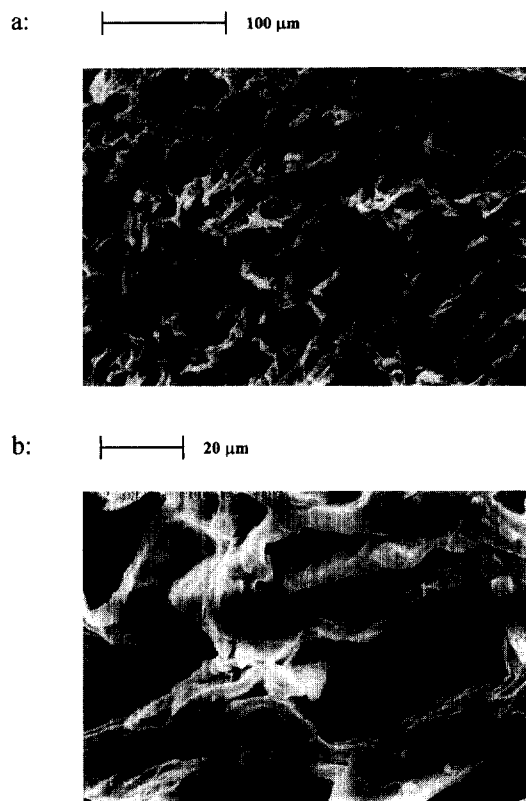


Figure 13 SEM micrographs at two different magnifications of blend PE/EMA 3/7 sheared during 125 min at $T = 180^{\circ}\text{C}$ and $\dot{\gamma} = 0.4\text{ s}^{-1}$

force increased with time during the first part of the test, due to the increase of molecular weight of the continuous EMA phase. At 160°C , a regular increase of these two parameters with time was observed up to 80 min, and no evolution of the morphology could be detected: the samples remained entirely soluble in chloroform, indicating that the PE domains were still dispersed in a continuous EMA matrix. We then increased the temperature up to 180°C and obtained the curves shown in Figure 12 for the torque and normal force at a shear rate of 0.4 s^{-1} . The normal force is found to level off after about 40 min, and decreases after about 80 min, where a slight decrease of the torque is also observed. From the viscosity data of the EMA phase as a function of reaction time (see relevant section) we can estimate the time when the phase inversion criterion given by equation (1) is met for the blend composition, temperature and shear rate of the experiment. At 180°C and 0.4 s^{-1} , we find a reaction time of the order of 100 min, close to the time where the normal force and torque begin to decrease. The sample was cooled after 125 min shearing, and Figure 13 shows the morphology obtained after solvent treatment at two different magnifications. Quite clearly, the structure has become co-continuous, which is confirmed by the fact that the sample is no longer entirely soluble in chloroform. On the other hand, the EMA phase remains soluble, which means that the reaction has been kept below the gel point. This is in contradiction with the estimation of gelation times from the crossover point of the dynamic moduli, which at 180°C was found to be around 40 min (see Figure 4). A possible explanation might be that the formation of the network can be delayed by the steady shear flow, whereas the experiments of Figure 4 were obtained at rest.

We could not reach our initial aim, which was to induce phase inversion by increasing the viscosity of the continuous phase during flow. However, the morphology changed from a dispersed structure to dual phase continuity, for a reaction time where the viscosity ratio roughly satisfies equation (1). Moreover, this morphological evolution seems to be related to a maximum in the torque and normal force measured on the blend.

CONCLUSIONS

The main conclusions of the present work may be summarized as follows.

The choice of our model reactive system allowed us to increase the viscosity of one phase in a controlled way, and on the other hand to analyse easily the blend morphology by selective solvent extraction. The initial morphologies of reactive blends disagree with the empirical phase inversion rule, equation (1), the low viscosity component remaining dispersed at much higher concentrations than predicted. On the other hand, the morphologies were found to be co-continuous over a broad range of composition, this type of morphology being apparently very stable during flow and annealing. Starting from a dispersion of the more viscous PE in the reactive EMA and increasing the viscosity of EMA with the transesterification reaction, the morphology actually changed at a viscosity ratio close to that predicted by equation (1), but the result was a co-continuous structure and not as expected a dispersion of EMA in PE. This result can also be related to the apparent stability found for co-continuous structures in this system. As an extension of the present study, the influence of interfacial tension should be investigated, which will require a change to the chemical nature of the non-reactive component. Finally, the viscoelastic properties of the initially dispersed non-reactive phase may also influence the observed morphological changes. Therefore, different PE samples with different molecular weight distributions and levels of long-chain branching will be used.

REFERENCES

1. Paul, D. R. and Barlow, J. W., *J. Macromol. Sci.—Rev. Macromol. Chem.*, 1980, **C18**, 109.
2. Sperling, L. H., *Interpenetrated Polymer Networks and Related Materials*. Plenum, New York, 1981, Ch. 2.
3. Miles, I. S. and Zurek, A., *Polym. Eng. Sci.*, 1988, **28**, 796.
4. Jordhamo, G. M., Manson, J. A. and Sperling, L. J., *Polym. Eng. Sci.*, 1986, **26**, 517.
5. Elemans, P. H. M., van Gisbergen J. G. M. and Meijer, H. E. M., in *Integration of Fundamental Polymer Science and Technology—2*, ed. P. J. Lemstra and L. A. Kleintjens. Elsevier Applied Science, London, 1988, p. 112.
6. Utracki, L. A., *J. Rheol.*, 1991, **35**, 1615.
7. Gubbels, F., Blacher, S., Vanlathem, E., Jérôme, R., Deltour, R., Brouers F. and Tyssie, P., *Macromolecules*, 1995, **28**, 1559.
8. Geuskens, G., *Europhysics Conference on Macromolecular Physics*, European Physical Society, Prague, Czech Republic, July 1995, p. SL11.
9. Molau, G. E., *J. Polym. Sci., Part A*, 1965, **3**, 1267.
10. Molau, G. E. and Keskkula, H., *Appl. Polym. Symp.* 1968, **7**, 35.
11. Freeguard, G. F. and Karmarkar, M., *J. Appl. Poly. Sci.*, 1971, **15**, 1649.
12. Lambla, M., Druz, J. and Bouilloux, A., *Polym. Eng. Sci.*, 1987, **27**, 1221.
13. Lyngaae-Jorgensen, J. and Utracki, L. A., *Makromol. Chem., Macromol. Symp.*, 1991, **48/49**, 189.
14. Winter, H. H. and Chambon, F., *Polym. Bull.*, 1985, **13**, 499.
15. Winter, H. H., Morganelli, P. and Chambon, F., *Macromolecules*, 1988, **21**, 523.
16. Muller, R., Gérard, E., Dugand, P., Rempp, P. and Gnanou, Y., *Macromolecules*, 1991, **24**, 1321.
17. Favis, B. D. and Chalifoux, J. P., *Polymer*, 1988, **29**, 1761.
18. Metelkin, V. I. and Blekht, V. S., *Kolloid Zh.*, 1984, **46**, 476.
19. Tomotika, S., *Proc. R. Soc. (London)*, 1935, **A150**, 322.
20. Kuhn, W., *Kolloid Z.*, 1953, **132**, 84.
21. Meijer, H. E. H. and Janssen, J. M. H., in *Mixing and Compounding—Theory and Practical Progress*, Vol. 4, Progress in Polymer Processing Series, ed. I. Manas-Zloczower and Z. Tadmor. Hanser Verlag, Munich, 1993, p. 60.
22. Utracki, L. A., *Polymer Alloys and Blends 2*. Hanser Verlag, Munich, 1989, p. 181.
23. Stone, H. A., Bentley, B. J. and Leal, L. G., *J. Fluid Mech.*, 1987, **167**, 241.